ACS AGRICULTURAL SCIENCE & TECHNOLOGY

pubs.acs.org/acsagscitech
Article

A New GH3 β-Glucosidase from *Chryseobacterium* sp. with Applications in Cellulosic Ethanol Production and Agri-Biotechnological Processes

Jessica Carvalho Bergmann, Valquiria Alice Michalczechen Lacerda, Kamila Lourrane Carvalho Alencar, Léia Cecília de Lima Fávaro, Dasciana de Sousa Rodrigues, Luis Fernando Marins, and Betania Ferraz Quirino*

Cite This: https://doi.org/10.1021/acsagscitech.5c01090

Read Online

ACCESS | Metrics & More | Article Recommendations | Supporting Information

ABSTRACT: β-Glucosidases catalyze the hydrolysis of β-glycosidic bonds and play key roles in biomass conversion and glycoside processing. We report the identification and characterization of Cr_B1, a GH3 β-glucosidase from *Chryseobacterium* sp. containing a predicted signal peptide. Cr_B1 hydrolyzed pNPG, cellobiose, salicin, and daidzin, showing optimal activity at pH 5.0−5.5 and 45−55 °C. The enzyme retained over 90% activity after 190 days at 4 °C and 25 °C and above 80% activity after 24 h at 50 °C, indicating remarkable long-term and thermal stability. Cr_B1 exhibited high glucose tolerance (IC_{50}: 1.5−1.8 M) and substrate-dependent kinetics. In synergy with Celluclast, it increased glucose release from CMC by 69%, demonstrating its potential to enhance enzymatic saccharification. These properties highlight Cr_B1 as a promising biocatalyst for improving saccharification, enhancing isoflavone bioavailability, and reducing bitterness in food and feed applications.

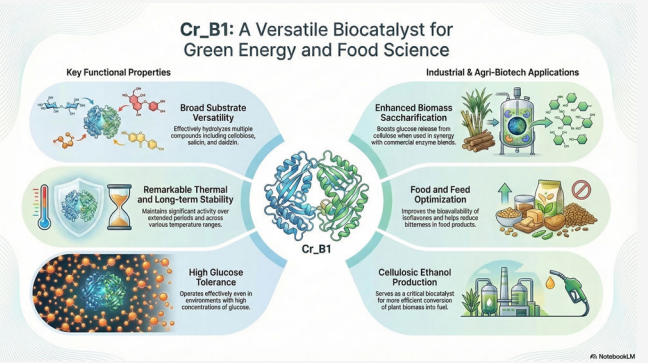

KEYWORDS: *beta-glucosidase, enzyme kinetics, hydrolysis, GH3 family, glucose tolerance, biomass saccharification*

1. INTRODUCTION

β-Glucosidases (EC3.2.1.21) are enzymes that play a crucial role in hydrolyzing β-1,4 glycosidic bonds found in β-D-glycosides, disaccharides, and oligosaccharides. These bonds are abundant in plant biomass, glycosides, and complex carbohydrates, making β-glucosidases essential for applications in bioenergy, agriculture, pharmaceuticals, and food processing.[1−3] In addition to their importance in biomass deconstruction, these enzymes contribute to the bioactivation of glycosylated compounds by increasing the bioavailability of flavonoids and phenolics, which are often bound to carbohydrate moieties. For instance, they convert salicin into salicylic acid, a precursor of anti-inflammatory drugs, and hydrolyze glycosylated isoflavones such as daidzin into daidzein, a compound with antioxidant and estrogenic properties.[4] In food and feed industries, β-glucosidases are also employed to hydrolyze bitter glycosides and enhance the nutritional and functional value of glycosylated bioactives.[5] Within this framework, β-glucosidases are recognized as pivotal constituents of enzymatic cocktails employed in cellulosic (2G) bioethanol production and a broad range of biomass-derived biotechnological applications.[6]

In industrial contexts, several characteristics are particularly desirable for β-glucosidases, including broad substrate specificity, high thermo and pH stability, and especially tolerance to glucose inhibition.[7] Their own reaction product, glucose, limiting their effectiveness under high-load saccharification conditions, inhibits many naturally occurring β-glucosidases. Enzymes that retain activity in the presence of high glucose concentrations are therefore of high interest for improving the efficiency and cost-effectiveness of biomass-to-sugar conversions.[8] The Carbohydrate Active Enzyme (CAZy) database (http://www.cazy.org/) classifies glycoside hydrolases (GH) into families based on amino acid sequence similarity. According to CAZy, β-D-glycosidase activity (EC3.2.1.21) is found in glycoside hydrolase families GH 1, 2, 3, 5, 16, 30, 39, 116, 131, 175, and 180.[9] In terms of catalytic mechanism, β-glucosidases can be classified

Received: November 27, 2025
Revised: May 6, 2026
Accepted: May 6, 2026

according to the hydrolysis of the substrate, glucosidic bond being hydrolyzed, and type of reaction.[7] Among the glycoside hydrolase families, GH3 β-glucosidases are known for their structural diversity and multifunctionality[10] and their active site comprising two domains.[7] However, most characterized members of this family originate from fungal or model bacterial species, and often exhibit limited substrate scope or sensitivity to glucose. Expanding the catalog of GH3 enzymes from underexplored microbial taxa is therefore essential for identifying novel biocatalysts with enhanced industrial properties.[11]

Members of the genus *Chryseobacterium* are widely distributed in diverse environments such as soil, water, plant-associated niches, and industrial settings. Several species have attracted biotechnological interest due to their ability to produce extracellular enzymes involved in the degradation of complex biomolecules, including proteases, lipases, and glycoside hydrolases, suggesting potential applications in biotechnology and bioprocessing.[5,12] The genus *Chryseobacterium* remains relatively uncharacterized in terms of glycoside hydrolase diversity, with only one β-glucosidase from *Chryseobacterium scophthalmum* described.[13] In this study, we present the biochemical characterization of Cr_B1, a novel GH3 β-glucosidase from *Chryseobacterium* sp., isolated from sugarcane field soil. This enzyme displays several features highly desirable for industrial application, including broad substrate specificity, significant glucose tolerance, thermostability, and strong synergy with commercial cellulases. This is the first report detailing the biochemical and enzymatic properties of a β-glucosidase from *Chryseobacterium* sp. originating from soil of a sugarcane field.

2. MATERIALS AND METHODS

2.1. Sequence Analysis

The Cr_B1 enzyme was identified from the genome of *Chryseobacterium* sp., isolated from sugarcane field soil (GenBank accession: PV741064). Its predicted amino acid sequence was analyzed using the ExPASy ProtParam tool to determine the extinction coefficient. Signal peptide prediction was performed with SignalP-6.0,[14] and functional domains and motifs were identified using InterProScan.[15] The Cr_B1 sequence was aligned with biochemically characterized GH3 β-glucosidases from UniProt.[16] A phylogenetic tree was constructed by aligning Cr_B1 with biochemically characterized and putative β-glucosidases identified via BLASTp (NCBI), using Clustal W[17] and MEGA X[18] with the Neighbor-Joining method[19] and 1000 bootstrap replicates.

2.2. Gene Cloning and Expression

The Cr_B1 gene was amplified from *Chryseobacterium* sp. genomic DNA using PCR with a forward primer (5′-GCTAGCATGAACAAGAACACATTTAC-3′), containing a NheI site, and a reverse primer (5′-CTCGAGTGGCTTCAGCTCGTTAAAC-3′), containing an XhoI site. The PCR product was cloned into the pET21a(+) vector (Novagen) between NheI and XhoI restriction sites and transformed into *E. coli* Tuner (DE3). Gene expression was carried out in 1 L baffled flasks containing Terrific Broth (TB)[20] at 37 °C and 250 rpm. When the culture reached an OD_{600} of 0.6, IPTG was added to a final concentration of 2 mM (200 μL of 1 M IPTG per 100 mL culture), and incubation continued at 18 °C for 48 h.

2.3. Protein Purification

The *E. coli* culture was centrifuged at 8000 × *g* for 10 min at 4 °C. The supernatant was filtered through a 0.45 μm PES membrane and the recombinant Cr_B1 protein, containing a C-terminal His-tag, was purified by immobilized metal affinity chromatography (IMAC) using a 5 mL GE His-Trap HP nickel column coupled to an ÄKTA Pure 25 M Chromatography System (Cytiva). Column equilibration and elution were performed using Lew buffer (50 mM NaH_2PO_4, 300 mM NaCl), with a linear gradient of 500 mM imidazole added for elution, following the Protino Ni-TED/IDA protocol (Cytiva). Collected fractions were analyzed by 12% SDS-PAGE[21] (4% stacking gel) and visualized by silver staining.[22] For Western blotting, proteins were transferred to a nitrocellulose membrane and detected using a monoclonal anti-His tag antibody.[23]

2.4. Enzyme Activity Assay

p-Nitrophenyl-β-D-glucopyranoside (pNPG) was used to monitor Cr_B1 gene expression, purification, and enzymatic activity. Reactions (100 μL total) contained 10 μL of 50 mM pNPG, 10 μL of diluted enzyme, 10 μL of UB4 buffer (pH 5.0),[24] and 70 μL of sterile Milli-Q water. After incubation at 50 °C for 15 min in a thermocycler, reactions were stopped with 100 μL of 2% (w/v) Na_2CO_3. The released *p*-nitrophenol (pNP) was quantified by absorbance at 405 nm using a SpectraMax M2 spectrophotometer (Molecular Devices), and enzyme activity was calculated from a pNP standard curve. One unit (U) of activity corresponds to the release of 1 μmol of pNP per minute under the assay conditions.[25]

2.5. Substrate Specificity

Substrate specificity of the Cr_B1 enzyme was evaluated by measuring its activity against various synthetic substrates, including pNPG (*p*-nitrophenyl-β-D-glucopyranoside), pNPGal (*p*-nitrophenyl-β-D-galactopyranoside), pNPC (*p*-nitrophenyl-β-D-cellobioside), pNPαG (*p*-nitrophenyl-α-D-glucopyranoside), and pNPX (*p*-nitrophenyl-β-D-xylopyranoside) at a final concentration of 5 mM. Reactions (100 μL) contained 10 μL of Cr_B1 (0.05 mg/mL), 10 μL of substrate stock solution (50 mM), 10 μL of UB4 buffer (pH 5.0), and 70 μL of sterile Milli-Q water. Controls used heat-inactivated enzyme. Reactions were performed in triplicate, incubated at 50 °C for 15 min, and stopped with 100 μL of 2% Na_2CO_3, and absorbance was measured at 405 nm.

For natural substrates (cellobiose, maltose, lactose, salicin, xylobiose (Sigma), and daidzin (Sellex Inc.)), activity was measured using glucose monoreagent (Bioclin). Reactions (100 μL) contained 20 μL of enzyme (0.1 mg/mL), 15 μL of substrate (150 mM), 30 μL of buffer, and 35 μL of water. Controls used heat-inactivated enzyme. Reactions were incubated at 50 °C for 30 min, stopped by heating at 95 °C, then incubated with 180 μL of glucose monoreagent at 37 °C for 15 min. Absorbance was read at 505 nm, and activity was expressed as U/mg.

2.6. Enzyme Properties

Enzyme property assays were performed using the best substrates identified in the specificity tests: pNPG, cellobiose, and salicin. Optimal pH was determined by measuring Cr_B1 activity at 50 °C across a pH range of 2.0−8.2 using the UB4 10 × X buffer system.[24] Reactions (100 μL) contained 10 μL of Cr_B1 (0.05 mg/mL for pNPG; 0.1 mg/mL for disaccharides), 10 μL of substrate (50 mM pNPG or 150 mM cellobiose/salicin), 10 μL of buffer, and 70 μL of sterile Milli-Q water. Controls used heat-inactivated enzyme.

For pNPG, reactions were incubated for 10 min and stopped with 100 μL of 2% Na_2CO_3; absorbance was measured at 405 nm. For disaccharides, reactions were incubated for 20 min and then stopped by heating at 95 °C. After cooling, 150 μL of glucose monoreagent (Bioclin) was added and incubated at 37 °C for 15 min; absorbance was measured at 505 nm. Enzyme activity was calculated using standard curves of pNP and glucose.

Optimal temperature was determined by performing the same reactions at the previously determined optimal pH for each substrate, across temperatures ranging from 20 to 70 °C. Reaction setup and controls remained the same.

https://doi.org/10.1021/acsagscitech.5c01090
ACS Agric. Sci. Technol. XXXX, XXX, XXX-XXX

2.7. Thermostability

Thermostability of the Cr_B1 enzyme was assessed using pNPG as substrate. The purified enzyme at a concentration of 0.01 mg/mL was incubated in buffer at the optimal pH of 5.5 at three different temperatures: 4 °C, 25 °C, and the optimal temperature for the substrate (i.e., 50 °C). Enzymatic activity assays were performed as previously described. Enzyme activity was monitored for 190 days to evaluate the long-term storage stability (shelf-life) of the enzyme.

2.8. Effect of Glucose on Cr_B1 Activity

To evaluate the effect of glucose on Cr_B1 activity, IC_{50} and K_i values were determined. For IC_{50}, enzyme activity was measured in the presence of glucose at concentrations ranging from 0 to 3 M. Activity was calculated based on a *p*-nitrophenol (pNP) standard curve, with 100% activity defined as the control without glucose.[26] Relative activity values were plotted to determine the IC_{50}. The inhibition constant (K_i) was determined by Lineweaver−Burk analysis to assess the type and degree of inhibition.[27,28] Data analysis was performed using GraphPad Prism v10.4.0 (GraphPad Software, Boston, MA, USA).

2.9. Kinetic Parameters

Kinetic parameters for the Cr_B1 enzyme were determined by measuring the hydrolysis rates of pNPG, cellobiose, and salicin, analyzed using the Michaelis−Menten equation.[29] Reactions were performed under standard conditions, with pNPG concentrations ranging from 1 to 8 mM, cellobiose concentrations from 2 to 50 mM, and salicin concentrations ranging from 0.25 to 6 mM. V_{max}, K_m, and k_{cat} were calculated using GraphPad Prism software (v.10.4.0) for Windows, GraphPad Software (Boston, MA, USA, www.graphpad.com). Catalytic efficiency (k_{cat}/K_m) was also determined.

Synergistic activity assays were performed using medium-viscosity carboxymethyl cellulose (CMC; C4888, Sigma-Aldrich, Brazil) as substrate, the commercial cellulase preparation Celluclast (from *Trichoderma reesei*, diluted 1:4000), and the purified β-glucosidase Cr_B1. Reaction mixtures (100 μL final volume) contained 1% (w/v) CMC in UB4 10 × buffer (pH 5.5), prepared from 20 μL of 2.5% CMC, 10 μL of buffer, 10 μL of Celluclast, and Milli-Q water to volume. The mixture was pre-incubated at 50 °C for 30 min to allow the generation of cello-oligosaccharides by the endo- and exoglucanases present in Celluclast. Subsequently, 10 μL of purified Cr_B1 (0.00371 mg) was added, replacing an equal volume of water, and incubations continued at 50 °C for approximately 18 h. Control reactions included: (i) Celluclast alone, (ii) Cr_B1 alone, and (iii) no enzyme, all under identical conditions. After incubation, 150 μL of glucose monoreagent (Bioclin) was added, followed by incubation for 15 min at 37 °C. Absorbance was measured at 505 nm, and glucose concentrations were calculated from a standard curve. Glucose release was expressed relative to the Celluclast-only condition (set to 100%). The synergistic effect was determined as the ratio between the glucose released by the combined reaction (Celluclast + Cr_B1) and the sum of the individual reactions.

3. RESULTS AND DISCUSSION

3.1. Sequence Analysis

This work marks the first characterization of Cr_B1, a GH3 β-glucosidase from a *Chryseobacterium* sp. isolated from sugarcane field soil. To date, the only β-glucosidase from this genus described in the literature is CsBGL, from *Chryseobacterium scophthalmum* 1433, which was reported by Yan et al.[13] as highly specific for cleaving the β-1,2-glucosidic bond in stevioside, leading to rubusoside production. A BLAST analysis comparing the amino acid sequences of Cr_B1 and *Chryseobacterium scophthalmum* revealed 30.98% identity over 78% coverage with 49% of similarity, clearly highlighting the divergence between the two sequences. Such a low level of identity, even with substantial coverage, strongly supports that Cr_B1 represents a distinct β-glucosidase rather than a close homolog. This degree of sequence variation is consistent with the observed biochemical differences, further emphasizing the novelty of Cr_B1 within the GH3 family.

The ORF of Cr_B1 encodes a protein of 819 amino acids, with a predicted molecular mass of 90.91 kDa and an extinction coefficient of 95,690 M^{-1} cm^{-1}. SignalP 6.0 analysis revealed a signal peptide at the N-terminus (cleavage site between residues 33−34; probability 0.9412), suggesting secretion via the Sec-dependent pathway.[30] Consistently, high enzyme activity was detected in the culture supernatant, supporting extracellular localization, an advantageous feature for biotechnological applications. InterProScan analysis identified Glyco_hydro_3, Glyco_hydro_3_C, and Fn3-like domain (Figure 1a) which are associated with catalysis and substrate recognition. Additionally, a C-terminal Fn3-like domain was identified, whose function is still under investigation. Recent studies indicate that this domain may enhance enzyme conformation, solubility, and activity.[31,32]

Multiple sequence alignment against GH3 β-glucosidases (UniProt) showed conserved motifs typical of GH3 β-glucosidases (Figure 1b), including TDW and KHF, which are essential for catalysis and substrate interaction. In the TDW motif, the aspartic acid (D) acts as the catalytic nucleophile.[33] Notably, while most GH3 enzymes possess an SDW sequence, Cr_B1 features a TDW motif, suggesting a potential structural or functional variation without altering the core catalytic mechanism.[34] The KHF motif likely contributes to enzyme stability and substrate recognition, with lysine (K) and histidine (H) involved in proton transfer, and phenylalanine (F) maintaining active site integrity.[34,35] Additionally, a conserved glutamic acid (E) serves as the acid/base catalyst for glycosidic bond hydrolysis, with all these residues strategically positioned to ensure efficient substrate binding and cleavage.[36] Structural studies of GH3 β-glucosidases from *Bifidobacterium adolescentis* have shown that residues such as Asp44 and Arg50 participate in hydrogen-bond interactions with hydroxyl groups of the glycone moiety.[37] In Cr_B1, the corresponding residues Asp131 and Arg137 are conserved, suggesting that similar interactions may occur within the catalytic pocket and contribute to substrate recognition.

A phylogenetic tree was constructed based on alignment with homologous sequences (Figure 2). Cr_B1 clustered in a tree branch with uncharacterized putative β-glucosidases, while six previously characterized GH3 β-glucosidases (marked with an asterisk) which are the same sequences used in the alignment, were dispersed throughout the tree. Although Cr_B1 shares 99.51% sequence identity with a putative β-glucosidase from *Chryseobacterium* sp. (WP_307451284.1), the strain used in this study was isolated from sugarcane plantation soil in the Brazilian Atlantic Forest, a biome known for its high biodiversity and humid tropical climate. These environmental conditions may influence microbial communities and drive enzymatic adaptations of biotechnological interest. Phylogenetic analysis (Figure 2) revealed close relationships with proteins from *Epilithonimonas* sp. and *Flavobacterium* sp., both members of the Flavobacteriaceae family (Bacteroidetes), involved in organic carbon cycling in aquatic ecosystems.[42,43] Although these related proteins lack experimental validation for β-glucosidase activity, the confirmed activity of Cr_B1 suggests functional conservation within this clade. BLASTp alignments revealed ~82% identity between Cr_B1 and both *Epilithonimonas* and *Flavobacterium* homologs. Sequence

https://doi.org/10.1021/acsagscitech.5c01090
ACS Agric. Sci. Technol. XXXX, XXX, XXX-XXX

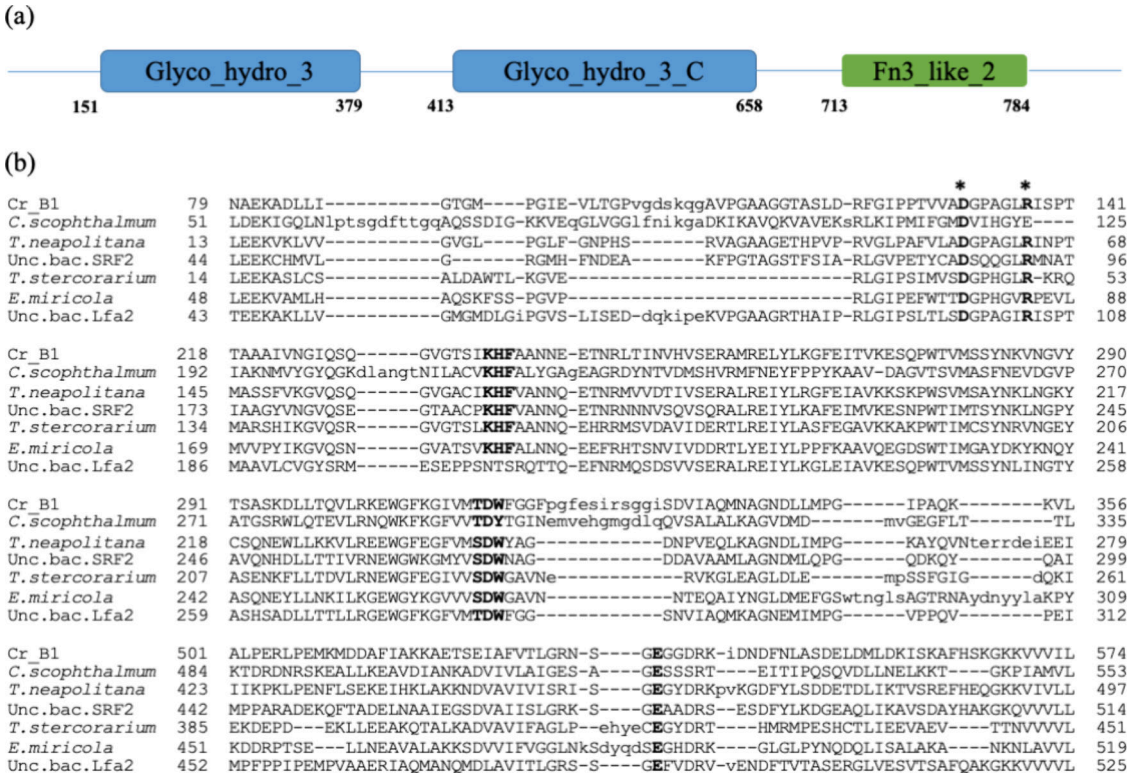

Figure 1. Domain analysis of Cr_B1 and partial alignment of β-glucosidases protein sequences. (a) The numbers indicate the start and end positions of the amino acid sequence for each domain. (b) A segment of the Cr_B1 protein aligned with β-glucosidases from different bacteria. Conserved positions in all GH3 β-glucosidases are shown in bold (KHF, T(S)DW, and E). The residues Asp131 (D) and Arg137 (R) in Cr_B1 that correspond to positions previously reported to interact with the glycone moiety in GH3 β-glucosidases are shown in bold and marked with an asterisk (*). Sequences homologous to Cr_B1 were from published papers that had biochemically characterized: *Thermotoga neapolitana* (ABI29899.1),[37] *Chryseobacterium scophthalmum* (QTA74163.1),[13] Uncultured bacterium SRF2 (AGH13475.1),[38] *Thermoclostridium stercorarium* (CAB08072),[39] *Elizabethkingia miricola* (AJW62880.1),[40] and uncultured bacterium Lfa2 (AXK90334.1).[41] Protein alignment was obtained with Uniprot.

diversity among β-glucosidases reflects evolutionary pressures, resulting in functional specialization and environmental adaptation.[44,45] While catalytic residues tend to be conserved, peripheral regions often vary to optimize enzyme performance under specific conditions such as pH, temperature, and substrate availability[46] (Table 1).

3.2. Gene Expression, Purification, and Substrate Specificity

The Cr_B1 gene was expressed and the enzyme purified for characterization. SDS-PAGE analysis (Figure 3) revealed a band between 70 and 100 kDa, consistent with the predicted size of 90.91 kDa corresponding to Cr_B1 via detection of its His-tag; a His-tagged protein was used as a positive control. Western blot analysis provided evidence of the protein's integrity, as no significant degradation products or non-specific bands were observed.

Substrate specificity of Cr_B1 was assessed using synthetic and natural substrates. Among the synthetic substrates (Figure 4a), Cr_B1 showed highest activity toward pNPG (14.9 U/mg) with lower activity against pNPX and pNPαG, and minimal or no activity with pNPGal and pNPC, respectively, indicating a preference for β-1,4-linked substrates with simple hydrolytic mechanisms (Figure 4a). For natural substrates (Figure 4b), Cr_B1 exhibited high activity with salicin (79.5 U/mg) and daidzin (95.1 U/mg), likely due to the more accessible glycosidic bonds in these compounds.[53,54] Its performance is comparable to other β-glucosidases, such as Bgl3B from *Talaromyces leycettanus*, which also acts on pNPG and isoflavone glycosides. Activity on cellobiose was approximately 56 U/mg, and negligible for lactose, maltose, and xylobiose. Based on these results, pNPG, salicin, and cellobiose were selected for further physicochemical and kinetic characterization experiments.

The substrate profile of Cr_B1 highlights its broad industrial potential, spanning biofuels, animal feed, and nutraceuticals. In bioethanol production, its ability to hydrolyze cellobiose into fermentable sugars and tolerate glucose reduces product inhibition during saccharification.[49,55] Its ability to hydrolyze daidzin, an isoflavone glycoside, converting it into daidzein -a phytoestrogen found in soybeans- highlights possible applications in the nutraceuticals industry, particularly in the development of functional products aimed at alleviating menopausal symptoms.[56] Additionally, Cr_B1 may enhance the bioavailability of antioxidant bioactives, supporting further uses in both food and feed industries.[55] The enzyme's origin, soil from a sugarcane field, may explain its adaptation to substrates such salicin and daidzin in addition to cellobiose. These environments are rich in plant residues (e.g., cellulose, hemicellulose, glycosides), which favor the evolution of β-glucosidases with

https://doi.org/10.1021/acsagscitech.5c01090
ACS Agric. Sci. Technol. XXXX, XXX, XXX-XXX

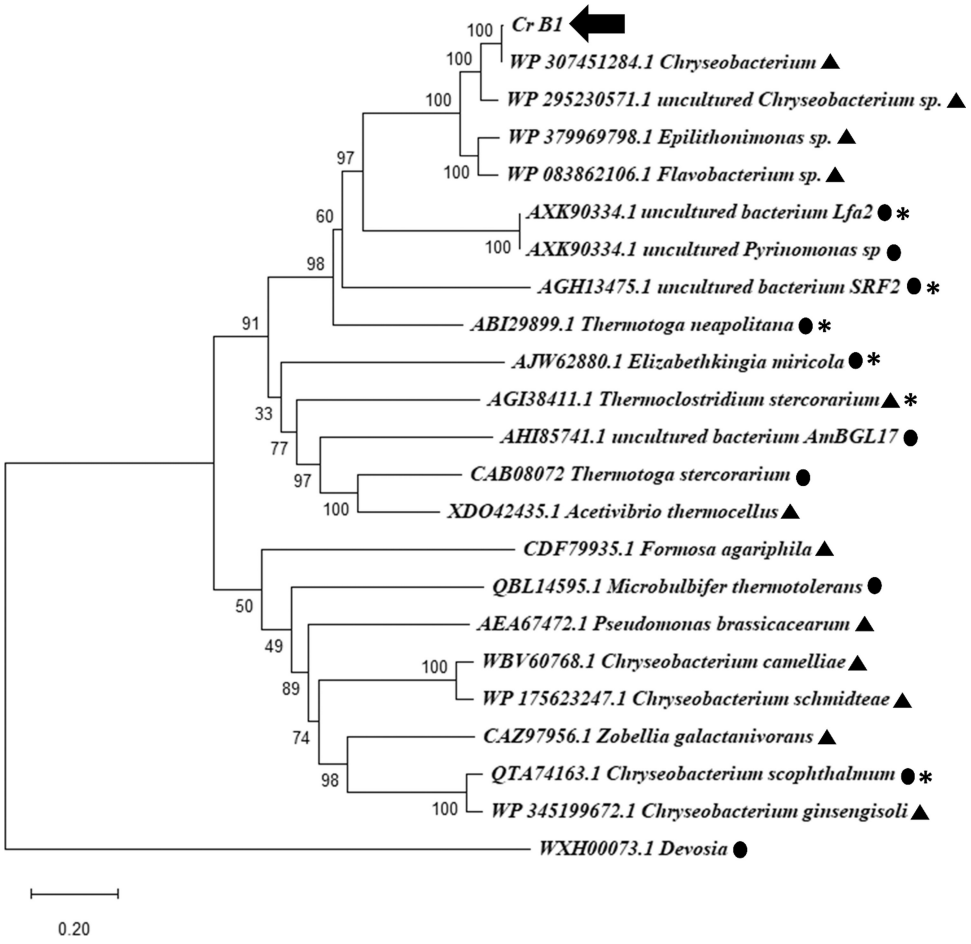

Figure 2. Phylogenetic tree showing GH3 β-glucosidases protein sequences from bacteria. Cr_B1 is indicated with an arrow. Sequences were chosen from Blastp results and GH3 sequences used in Figure 1 were also included and are marked with *. Putative sequences are marked with black triangles and characterized sequences are marked with black circles. Accession numbers (NCBI or PDB accession code) are shown before each sequence. *Devosia* sp., a β-glucosidase GH1, was used as the outgroup. The percentage of replicate trees in which the associated taxa clustered together in the bootstrap test (1000 replicates) are shown next to the branches. The evolutionary distance using MEGAX software was computed using the Poisson correction method and are in the units of the number of amino acid substitutions per site.

broad specificity for diverse plant-derived compounds.[57,58] Such microbial niches represent promising reservoirs of novel biomass-degrading enzymes with industrial relevance.

3.3. Physicochemical Characterization and Kinetic Parameters

Cr_B1 exhibited optimal activity for pNPG within a broad range of moderate temperatures (45−55 °C), suggesting that the enzyme maintains activity across different thermal conditions (Figure 4c). For cellobiose and salicin, optimal temperatures were 50 °C and 45 °C, respectively. The lower optimum observed for salicin may suggest subtle differences in enzyme−substrate interaction dynamics. Regarding pH (Figure 4d), maximum activity occurred at pH 5.0 for pNPG and at pH 5.5 for both salicin and cellobiose, which agrees with the values commonly reported for bacterial and metagenomic GH3 β-glucosidases, which generally display activity within a broad pH range of 3−7 (Table 1). The slight shift toward pH 5.5 for natural substrates such as salicin and cellobiose may reflect an increased affinity for glycosidic bonds in more complex molecules.

Cr_B1 exhibited remarkable stability under both refrigerated (4 °C) and ambient (25 °C) conditions. The enzyme retained more than 95% of its activity at 25 °C for 190 days, highlighting its exceptional long-term stability at room temperature. This level of stability is advantageous for extended storage, which is a key requirement for industrial processes, ultimately contributing to cost reduction, logistical efficiency, and improved process reliability. Such robustness enhances Cr_B1's potential for diverse applications, including cellulosic ethanol production, enhancement of isoflavone bioavailability, and food or feed processing. Notably, its sustained activity under both refrigerated and ambient conditions represents a significant advantage over many β-glucosidases reported in the literature, which typically lose activity more rapidly under similar conditions.[11] In contrast, the enzyme showed limited stability at higher temperatures, behaving as commonly observed for GH3 β-glucosidases. Nevertheless, its residual activity at elevated temperatures suggests it could still be effective in short-duration processes, such as batch hydrolysis or enzymatic food treatment, especially when substrate stabilization occurs. For example, *Lactobacillus paracasei* β-glucosidase retained

https://doi.org/10.1021/acsagscitech.5c01090
ACS Agric. Sci. Technol. XXXX, XXX, XXX-XXX

Table 1. Biochemical Characteristics of Microbial β-Glucosidases from Different Environments

microorganism	name	substrate	opt. temp. °C	opt. pH	V_{max} (U/mg)	K_m (mM)	k_{cat} (s^{-1})	k_{cat}/K_m (mM^{-1} s^{-1})	ref
Levilactobacillus brevis	Bglb	pNPG	37	7	77 μM min^{-1}	0.22	60	NI[a]	Bockwoldt and Ehrmann[47]
Leifsonia sp. ZF2019	Bgl1973	pNPG	50	7	44.44	0.22	57.78	262.6	He et al.[48]
metagenome	Lfa2	pNPG	50	5.5	9.4	0.76	13.2	0.0174	Alves et al.[41]
Chyseobacterium sp.	Cr_B1	pNPG	45-50-55	5	19.46	0.38	0.3243	0.8534	this work
metagenome	LAB25g2	pNPG	50	4.5-5.5	1.5	0.45	0.41	9.2	Del Pozo et al.[38]
Lactobacillus paracasei	LpBgla	pNPG	30	5.5	NI*	3.61	3.982	2.765	Xie et al.[49]
Marinomonas MWYL1	NI*	cellobiose	40	7	367	1.1	435	395.8	Zhao et al.[50]
Chyseobacterium sp.	Cr_B1	cellobiose	50	5.5	0.7869	6.805	0.01339	0.00196	this work
Thermoanaerobacterium xylanolyticum	TxGH116	cellobiose	75	5.5	13.4	0.203	36.1	178	Pengthaisong et al.[51]
	D593A		70	6	0.000345	0.255	0.00167	0.00655	
	D593N		70	7	0.000336	0.284	0.00146	0.00514	
metagenome	Lfa2	cellobiose	50	5.5	16.2	75.3	22.8	0.0302	Alves et al.[41]
metagenome	LAB25g2	cellobiose	50	4.5-5.5	1537.2	4.88	0.1	20.84	Del Pozo et al.[38]
Chyseobacterium sp.	Cr_B1	salicin	45	5.5	18.55	0.776	0.3124	0.4024	this work
Lactobacillus lactis NZ9000/ pMG36e-usp45	bglA	salicin	50	7	1343	38.61	434.8	11.26	Wang et al.[52]
	bglB				1254	43.99	b	7.93	
	bgl				1347	34.8	1016	29.2	
Lactobacillus paracasei	LpBgla	salicin	30	5.5	58.32 uM min^{-1}	2.25	2.973	1.321	Xie et al.[49]

[a]NI: No Information.

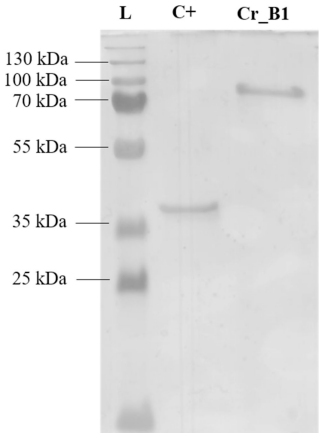

Figure 3. Cr_B1 protein purification analysis. 12% SDS-PAGE. L-PageRuler Prestained Protein Ladder; C + is a His-tag containing protein used as a positive control; Cr_B1 purified with the size of 90.91 kDa.

full activity only for 2 h at 20−30 °C,[49] and a GH3 enzyme from a soda lake metagenome remained ~70% active for 16 h at 37 °C.[11] These results suggest that Cr_B1 is a mesophilic enzyme with cold-adapted features, potentially due to conformational flexibility or cold-induced stabilization. For applications requiring thermal resistance, strategies such as protein engineering or immobilization may be needed.[2]

Thermostability analysis (Figure 5a) showed that at 50 °C, enzyme activity dropped to ~60% within 1.5 days and after 3 days, its activity was completely lost. In contrast, Cr_B1 remained highly stable at 4 °C and 25 °C, maintaining over 90% activity for 190 days. This long-term stability during storage may also be associated with structural features commonly observed in GH3 β-glucosidases. These enzymes often present a multidomain architecture that contributes to structural rigidity, and accessory domains such as fibronectin type III (FnIII) have been suggested to participate in structural stabilization or substrate interactions, which may help preserve enzyme integrity over prolonged storage periods.[32] Many β-glucosidases reported in the literature show lower stability than Cr_B1 under comparable conditions. For example, a β-glucosidase from *Lactobacillus paracasei* retained full activity after incubation at 20−30 °C but showed reduced activity at temperatures approaching 50 °C,[49] while a GH3 β-glucosidase from a soda lake metagenomic library maintained more than 70% activity for 16 h at 37 °C but decreased stability at higher temperatures.[11] These observations indicate that Cr_B1 behaves as a typical mesophilic β-glucosidase. The rapid inactivation observed at 50 °C may be associated with temperature-induced conformational destabilization affecting the catalytic site and substrate-binding interactions.[59] From an applied perspective, strategies such as protein engineering or enzyme immobilization may help improve the thermal stability of Cr_B1 for industrial applications.[2]

Kinetic analysis (Table 1) revealed high catalytic efficiency for pNPG (k_{cat}/K_m: 0.8534 $mM^{-1}{\cdot}s^{-1}$), followed by salicin (0.4024 $mM^{-1}{\cdot}s^{-1}$), and low efficiency for cellobiose (0.00196 $mM^{-1}{\cdot}s^{-1}$), consistent with its higher K_m (6.805 mM). The kinetic profile of Cr_B1 indicates a preference for aryl-glucosides over disaccharides, with catalytic efficiency being highest for pNPG (k_{cat}/K_m = 0.85 $mM^{-1}{\cdot}s^{-1}$), intermediate for salicin (0.40 $mM^{-1}{\cdot}s^{-1}$), and very low for cellobiose (0.00196 $mM^{-1}{\cdot}s^{-1}$). This substrate-dependent pattern agrees with previous findings for GH3 β-glucosidases, which are generally more effective on synthetic aryl-glucosides than on natural

https://doi.org/10.1021/acsagscitech.5c01090
ACS Agric. Sci. Technol. XXXX, XXX, XXX-XXX

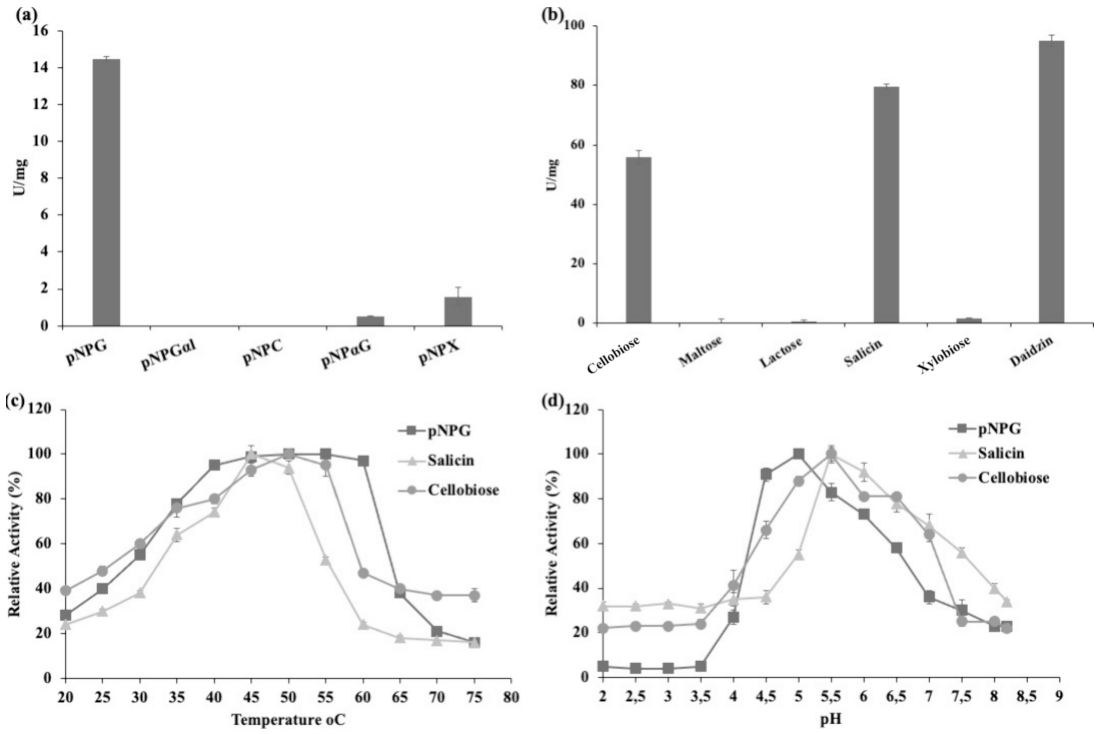

Figure 4. Cr_B1 enzyme substrate specificity and effect of pH and temperature. Specific activity (U/mg) of the Cr_B1 enzyme with synthetic substrates (a). Synthetic substrates were pNPG (*p*-nitrophenyl-β-D-glucopyranoside), pNPGal (*p*-nitrophenyl-β-D-galactopyranoside), pNPC (*p*-nitrophenyl-β-D-cellobioside), pNPαG (*p*-nitrophenyl-α-D-glucopyranoside), and pNPX (*p*-nitrophenyl-β-D-xylopyranoside). (b) Specific activity (U/mg) of the Cr_B1 enzyme with natural substrates cellobiose, maltose, lactose, salicin, xylobiose, and daidzin. Error bars represent the standard deviation of three experiments. Effect of pH (c) and temperature (d) on the relative Cr_B1 enzyme activity. Substrates used were using pNPG (*p*-nitrophenyl-β-Dglucopyranoside), salicin, and cellobiose. Data points represent the mean of three independent experiments, with error bars indicating the standard deviation.

disaccharides. Furthermore, the moderate affinity observed for pNPG (K_m = 0.38 mM) is comparable to that of *Oenococcus oeni* ST81 and notably higher than that reported for *Lactobacillus plantarum* (1.82 mM), reinforcing that Cr_B1 displays kinetic features within the expected range for bacterial β-glucosidases while still showing distinct substrate preferences.[60,61] However, its overall efficiency is lower than highly active enzymes such as *Marinomonas* MWYL1 (500.5 $mM^{-1}{\cdot}s^{-1}$).[50] For cellobiose, the high K_m (6.805 mM) and low efficiency indicate poor substrate affinity. Structural studies of GH3 β-glucosidases suggest that this behavior may be related to the architecture of the catalytic pocket. For example, the crystal structure of BaBgl3 from *Bifidobacterium adolescentis* revealed that GH3 enzymes generally possess relatively shallow active-site pockets, which favor the hydrolysis of small soluble substrates rather than longer oligosaccharides such as cellobiose.[62] These structural features may help explain the higher catalytic efficiency of Cr_B1 toward aryl-glucosides such as pNPG and salicin while maintaining low activity toward cellobiose. Additionally, its performance with salicin suggests potential for hydrolyzing glycosides in industrial applications.

3.4. Glucose Tolerance and Inhibition Constant (K_i)

Glucose tolerance of Cr_B1 was assessed using pNPG at 50 °C and pH 5 (Figure 5b). Enzyme activity without glucose was set as 100%. A slight increase in activity was observed at 0.1 M glucose, followed by progressive inhibition at higher concentrations. Cr_B1 demonstrates remarkable glucose tolerance, maintaining activity even at glucose concentrations of 1.5−1.8 M (IC_{50}), a desirable trait for biofuel and food-processing contexts.[53] Lineweaver−Burk plots (Figure S1) plots demonstrate that with higher inhibitor concentrations (glucose), the lines diverge from the control, indicating a significant impact of glucose on enzyme kinetics. All lines converge at the Y-axis intercept, suggesting that the maximum velocity (V_{max}) remains unchanged. However, the *X*-axis intercept shifts as the inhibitor concentration increases, reflecting an increase in the Michaelis constant (K_m). This indicates that Cr_B1 enzyme affinity for the substrate decreases in the presence of glucose. The increased slope of the lines with higher inhibitor concentrations confirms that the inhibition follows a competitive mechanism. The inhibition constant (K_i) of Cr_B1 was calculated with the GraphPad Prim Software and determined to be 0.133 M, indicating a high affinity of the glucose inhibitor to the enzyme.

3.5. Synergistic Effect of β-glucosidase Cr_B1 on Cellulase from *Thichoderma reesei* (Celluclast)

The synergistic interaction between the commercial cellulase Celluclast (1:4000), derived from *Trichoderma reesei*, and the candidate enzyme Cr_B1 was evaluated using 1% medium-viscosity carboxymethylcellulose (CMC) as substrate. As shown in Figure 6, the combination of Celluclast and Cr_B1 released ∼169% relative glucose compared to the reaction with Celluclast alone (set as 100%). Reactions containing Cr_B1 alone or Celluclast in the absence of substrate showed minimal glucose release, indicating that Cr_B1 requires the prior action of cellulases to exert its effect. These results confirm a synergistic effect between

https://doi.org/10.1021/acsagscitech.5c01090
ACS Agric. Sci. Technol. XXXX, XXX, XXX-XXX

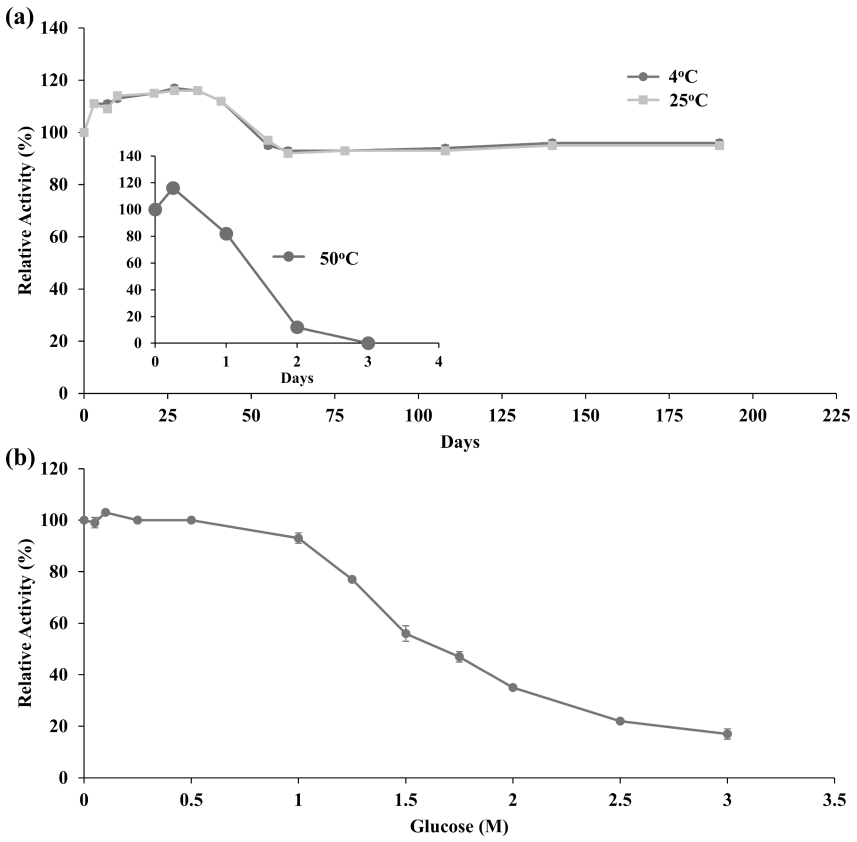

Figure 5. Thermostability and tolerance to glucose of Cr_B1 using pNPG as a substrate. (a) Thermostability was evaluated at 4 °C, 25 °C, and 50 °C using pNPG (*p*-nitrophenyl-β-D-glucopyranoside) as the substrate at optimum pH of 5. Data points represent the mean of three independent experiments, with error bars indicating the standard deviation. (b) The IC_{50} was approximately 1.5 M. The experiment was performed in triplicate, and error bars represent the standard deviation.

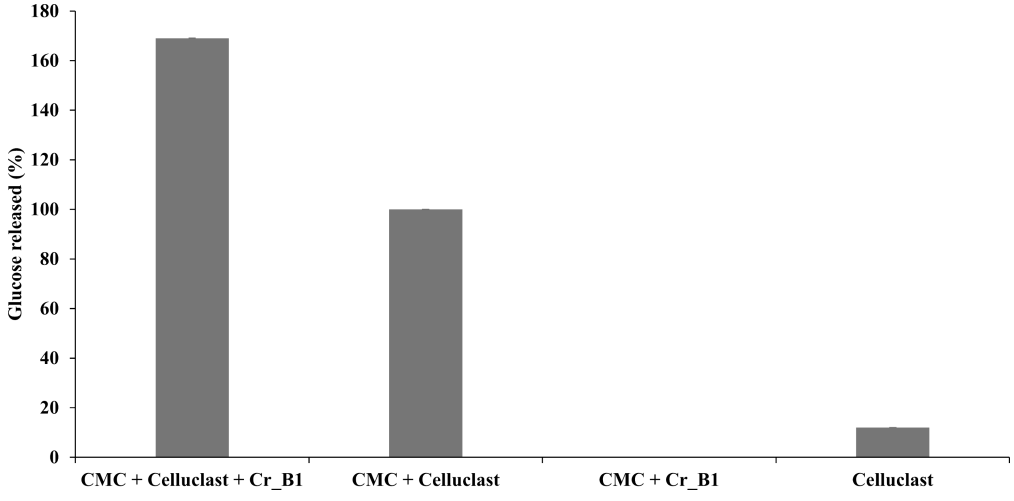

Figure 6. Synergistic effect of Cr_B1 on commercial Celluclast cellulase cocktail. Reactions were carried out using 1% medium-viscosity carboxymethyl cellulose (CMC) as substrate. Celluclast was diluted 1:4000, and Cr_B1 was used at 0.0037 mg per reaction. Data represent the mean of triplicates ± standard deviation.

the enzymes, with Cr_B1 increasing glucose release by ∼69% relative to Celluclast alone.

β-Glucosidases catalyze the final step of cellulose degradation by hydrolyzing cello-oligosaccharides, such as cellobiose, into glucose, thereby enhancing sugar yield and reducing product inhibition of upstream cellulases.[63] This function is critical in saccharification processes, where oligosaccharide accumulation can hinder enzymatic efficiency. The observed synergy highlights

https://doi.org/10.1021/acsagscitech.5c01090
ACS Agric. Sci. Technol. XXXX, XXX, XXX-XXX

Cr_B1's role in complementing commercial enzyme blends deficient in β-glucosidase activity, reinforcing its potential for improving saccharification efficiency.

3.6. Structural Implications and Engineering Prospects

Glucose tolerance in β-glucosidases is more commonly reported in GH1 enzymes, whereas most GH3 β-glucosidases are inhibited by glucose due to the easier access of the product to the catalytic pocket.[64] Structural studies indicate that GH1 enzymes possess deeper and narrower active-site cavities, while GH3 enzymes typically have a more exposed catalytic pocket that facilitates product inhibition.[64] However, structural variations in the catalytic channel may modulate glucose accessibility. For instance, comparative structural analyses of the glucose-tolerant MpBgl3 revealed that residues at the entrance of the catalytic channel can alter its geometry and electrostatic environment, restricting glucose access to the active site.[65] Similarly, molecular docking studies of the glucose-tolerant GH3 enzyme Bgl1973 suggested that residues such as Asp43, Lys151, His152, and Arg162 may participate in glucose interactions within the catalytic pocket.[48] In agreement with these observations, sequence alignment showed that Cr_B1 conserves residues previously implicated in glucose interaction and substrate recognition in GH3 β-glucosidases (Figure 1B), suggesting that similar structural features may contribute to the high glucose tolerance observed for this enzyme. Future studies combining homology modeling, structural analysis, and site-directed mutagenesis will be valuable to validate these hypotheses and guide the rational engineering of GH3 β-glucosidases with improved catalytic properties. Cr_B1 is a GH3 β-glucosidase from *Chryseobacterium* sp., successfully expressed in *E. coli* and secreted due to its native signal peptide. The enzyme shows remarkable stability, retaining >95% activity for 190 days at 25 °C, which favors storage and reduces operational costs. In addition to this stability, Cr_B1 efficiently hydrolyzes cellobiose, salicin, and daidzin, while maintaining glucose tolerance. These combined properties support its use in cellulosic ethanol production, pharmaceutical isoflavone enhancement, and flavor modulation in foods and beverages.

■ ASSOCIATED CONTENT

Data Availability Statement

Data was deposited on GenBank, under accession number: PV741064.

Supporting Information

The Supporting Information is available free of charge at https://pubs.acs.org/doi/10.1021/acsagscitech.5c01090.

Additional kinetic analyses of Cr_B1. This comprises the Lineweaver−Burk plot illustrating the effect of increasing glucose concentrations on enzyme activity, using pNPG (*p*-nitrophenyl-β-D-glucopyranoside) as substrate at 50 °C and pH 5 (Figure S1) (DOCX)

■ AUTHOR INFORMATION

Corresponding Author

Betania Ferraz Quirino − *Genetics and Biotechnology Laboratory, Embrapa Agroenergy, Brasília, DF 70770-901, Brazil;* orcid.org/0000-0002-7578-6314; Email: betania.quirino@embrapa.br; bfq@uwalumni.com. Tel.: +556134487115. Fax: +556132743127

Authors

Jessica Carvalho Bergmann − *Genetics and Biotechnology Laboratory, Embrapa Agroenergy, Brasília, DF 70770-901, Brazil*

Valquiria Alice Michalczechen Lacerda − *Genetics and Biotechnology Laboratory, Embrapa Agroenergy, Brasília, DF 70770-901, Brazil*

Kamila Lourrane Carvalho Alencar − *Genetics and Biotechnology Laboratory, Embrapa Agroenergy, Brasília, DF 70770-901, Brazil*

Léia Cecília de Lima Fávaro − *Genetics and Biotechnology Laboratory, Embrapa Agroenergy, Brasília, DF 70770-901, Brazil*

Dasciana de Sousa Rodrigues − *Genetics and Biotechnology Laboratory, Embrapa Agroenergy, Brasília, DF 70770-901, Brazil*

Luis Fernando Marins − *Molecular Biology Laboratory, Institute of Biological Sciences, Universidade Federal de Rio Grande (FURG), Rio Grande, RS 96203-900, Brazil*

Complete contact information is available at: https://pubs.acs.org/doi/10.1021/acsagscitech.5c01090

Author Contributions

CRediT J.C.B.: Investigation, Fromal analysis, Writing − Original Draft, Writing − Review and Editing. V.A.M.L.: Investigation. K.L.C.A.: Investigation. L.C.d.L.F.: Resources. D.d.S.R.: Validation. L.F.M.: Conceptualization, Funding acquisition. B.F.Q.: Conceptualization, Resources, writing − Review and editing, Supervision.

Funding

The Article Processing Charge for the publication of this research was funded by the Coordenacao de Aperfeicoamento de Pessoal de Nivel Superior (CAPES), Brazil (ROR identifier: 00x0ma614). This work was supported by the National Council for Scientific and Technological Development (CNPq), Research Support Foundation (FAP-DF), and Coordination for the Improvement of Higher Education Personnel (CAPES).

Notes

During the preparation of this work, authors used ChatGPT to improve readability of the manuscript. After using ChatGPT, the authors reviewed and edited the content as needed and take full responsibility for the content of the published article.
The authors declare no competing financial interest.

■ ACKNOWLEDGMENTS

The authors thank the Embrapa CLP for helpful comments and CNPq and FAP-DF for funding and fellowships.

■ REFERENCES

(1) Ketudat Cairns, J. R.; Esen, A. β-Glucosidases. *Cell. Mol. Life Sci.* **2010**, *67* (20), 3389–3405.

(2) Singh, G.; Verma, A. K.; Kumar, V. Catalytic Properties, Functional Attributes and Industrial Applications of β-Glucosidases. *3 Biotech.* **2016**, *6* (1), No. 3.

(3) Magwaza, B.; Amobonye, A.; Pillai, S. Microbial β-Glucosidases: Recent Advances and Applications. *Biochimie* **2024**, *225*, 49–67.

(4) De Morais Souto, B.; Florentino Barbosa, M.; Marinsek Sales, R. M.; Conessa Moura, S.; De Rezende Bastos Araújo, A.; Ferraz Quirino, B. The Potential of β-Glucosidases for Aroma and Flavor Improvement in the Food Industry. *Microbe* **2023**, *1*, No. 100004.

(5) Muradova, M.; Proskura, A.; Canon, F.; Aleksandrova, I.; Schwartz, M.; Heydel, J.-M.; Baranenko, D.; Nadtochii, L.; Neiers, F. Unlocking Flavor Potential Using Microbial β-Glucosidases in Food Processing. *Foods* **2023**, *12* (24), No. 4484.
(6) Paventi, G.; Di Martino, C.; Coppola, F.; Iorizzo, M. β-Glucosidase Activity of Lactiplantibacillus Plantarum: A Key Player in Food Fermentation and Human Health. *Foods* **2025**, *14* (9), No. 1451.
(7) Kannan, P.; Shafreen M, M.; Achudhan, A. B.; Gupta, A.; Saleena, L. M. A Review on Applications of β-Glucosidase in Food, Brewery, Pharmaceutical and Cosmetic Industries. *Carbohydr. Res.* **2023**, *530*, No. 108855.
(8) Kamale, C.; Rauniyar, A.; Bhaumik, P. Rational Design Facilitates the Improvement of Glucose Tolerance and Catalytic Properties of a B-glucosidase from *Acetivibrio Thermocellus*. *FEBS J.* **2025**, *292* (5), 1174–1196.
(9) Cantarel, B. L.; Coutinho, P. M.; Rancurel, C.; Bernard, T.; Lombard, V.; Henrissat, B. The Carbohydrate-Active EnZymes Database (CAZy): An Expert Resource for Glycogenomics. *Nucleic Acids Res.* **2009**, *37* (suppl_1), D233–D238.
(10) The CAZypedia ConsortiumTen Years of CAZypedia: A Living Encyclopedia of Carbohydrate-Active Enzymes. *Glycobiology* **2018**, *28* (1), 3–8.
(11) Jeilu, O.; Alexandersson, E.; Johansson, E.; Simachew, A.; Gessesse, A. A Novel GH3-β-Glucosidase from Soda Lake Metagenomic Libraries with Desirable Properties for Biomass Degradation. *Sci. Rep.* **2024**, *14* (1), No. 10012.
(12) Liu, X.; Wang, D.; Yin, Z.; Sun, L.; Pang, S.; Liu, J.; Li, W.; Cui, S.; Huang, W.; Du, Y.; Xie, Z. Insights into Evolutionary, Genomic, and Biogeographic Characterizations of *Chryseobacterium nepalense* Represented by a Polyvinyl Alcohol-Degrading Bacterium, AC3. *Microbiol. Spectrum* **2022**, *10* (5), No. e02179-22.
(13) Yan, Z.; Cao, X.; Yang, X.; Yang, S.; Xu, L.; Jiang, X.; Xiao, M. A Novel β-Glucosidase From *Chryseobacterium scophthalmum* 1433 for Efficient Rubusoside Production From Stevioside. *Front. Microbiol.* **2021**, *12*, No. 744914.
(14) Teufel, F.; Almagro Armenteros, J. J.; Johansen, A. R.; Gíslason, M. H.; Pihl, S. I.; Tsirigos, K. D.; Winther, O.; Brunak, S.; von Heijne, G.; Nielsen, H. SignalP 6.0 Predicts All Five Types of Signal Peptides Using Protein Language Models. *Nat. Biotechnol.* **2022**, *40* (7), 1023–1025.
(15) Blum, M.; Andreeva, A.; Florentino, L. C.; Chuguransky, S. R.; Grego, T.; Hobbs, E.; Pinto, B. L.; Orr, A.; Paysan-Lafosse, T.; Ponamareva, I.; Salazar, G. A.; Bordin, N.; Bork, P.; Bridge, A.; Colwell, L.; Gough, J.; Haft, D. H.; Letunic, I.; Llinares-López, F.; Marchler-Bauer, A.; Meng-Papaxanthos, L.; Mi, H.; Natale, D. A.; Orengo, C. A.; Pandurangan, A. P.; Piovesan, D.; Rivoire, C.; Sigrist, C. J. A.; Thanki, N.; Thibaud-Nissen, F.; Thomas, P. D.; Tosatto, S. C. E.; Wu, C. H.; Bateman, A. InterPro: The Protein Sequence Classification Resource in 2025. *Nucleic Acids Res.* **2025**, *53* (D1), D444–D456.
(16) The UniProt Consortium, Bateman, A.; Martin, M.-J.; Orchard, S.; Magrane, M.; Ahmad, S.; Alpi, E.; Bowler-Barnett, E. H.; Britto, R.; Bye-A-Jee, H.; Cukura, A.; Denny, P.; Dogan, T.; Ebenezer, T.; Fan, J.; Garmiri, P.; da Costa Gonzales, L. J.; Hatton-Ellis, E.; Hussein, A.; Ignatchenko, A.; Insana, G.; Ishtiaq, R.; Joshi, V.; Jyothi, D.; Kandasaamy, S.; Lock, A.; Luciani, A.; Lugaric, M.; Luo, J.; Lussi, Y.; MacDougall, A.; Madeira, F.; Mahmoudy, M.; Mishra, A.; Moulang, K.; Nightingale, A.; Pundir, S.; Qi, G.; Raj, S.; Raposo, P.; Rice, D. L.; Saidi, R.; Santos, R.; Speretta, E.; Stephenson, J.; Totoo, P.; Turner, E.; Tyagi, N.; Vasudev, P.; Warner, K.; Watkins, X.; Zaru, R.; Zellner, H.; Bridge, A. J.; Aimo, L.; Argoud-Puy, G.; Auchincloss, A. H.; Axelsen, K. B.; Bansal, P.; Baratin, D.; Batista Neto, T. M.; Blatter, M.-C.; Bolleman, J. T.; Boutet, E.; Breuza, L.; Gil, B. C.; Casals-Casas, C.; Echioukh, K. C.; Coudert, E.; Cuche, B.; de Castro, E.; Estreicher, A.; Famiglietti, M. L.; Feuermann, M.; Gasteiger, E.; Gaudet, P.; Gehant, S.; Gerritsen, V.; Gos, A.; Gruaz, N.; Hulo, C.; Hyka-Nouspikel, N.; Jungo, F.; Kerhornou, A.; Le Mercier, P.; Lieberherr, D.; Masson, P.; Morgat, A.; Muthukrishnan, V.; Paesano, S.; Pedruzzi, I.; Pilbout, S.; Pourcel, L.; Poux, S.; Pozzato, M.; Pruess, M.; Redaschi, N.; Rivoire, C.; Sigrist, C. J. A.; Sonesson, K.; Sundaram, S.; Wu, C. H.; Arighi, C. N.; Arminski, L.; Chen, C.; Chen, Y.; Huang, H.; Laiho, K.; McGarvey, P.; Natale, D. A.; Ross, K.; Vinayaka, C. R.; Wang, Q.; Wang, Y.; Zhang, J. UniProt: The Universal Protein Knowledgebase in 2023. *Nucleic Acids Res.* **2023**, *51* (D1), D523–D531.
(17) Thompson, J. D.; Higgins, D. G.; Gibson, T. J. CLUSTAL W: Improving the Sensitivity of Progressive Multiple Sequence Alignment through Sequence Weighting, Position-Specific Gap Penalties and Weight Matrix Choice. *Nucleic Acids Res.* **1994**, *22* (22), 4673–4680.
(18) Kumar, S.; Stecher, G.; Li, M.; Knyaz, C.; Tamura, K. MEGA X: Molecular Evolutionary Genetics Analysis across Computing Platforms. *Mol. Biol. Evol.* **2018**, *35* (6), 1547–1549.
(19) Saitou, N.; Nei, M. The Neighbor-Joining Method: A New Method for Reconstructing Phylogenetic Trees. *Mol. Biol. Evol.* **1987**, DOI: 10.1093/oxfordjournals.molbev.a040454.
(20) Sparrow, I.; Burgess, S. J. *Terrific Broth Medium V1*. Springer Nature; preprint; **2024**, DOI: 10.17504/protocols.io.x54v9pb24g3e/v1.
(21) Laemmli, U. K. Cleavage of Structural Proteins during the Assembly of the Head of Bacteriophage T4. *Nature* **1970**, *227* (5259), 680–685.
(22) Nesterenko, M. V.; Tilley, M.; Upton, S. J. A Simple Modification of Blum's Silver Stain Method Allows for 30 Minite Detection of Proteins in Polyacrylamide Gels. *J. Biochem. Biophys. Methods* **1994**, *28* (3), 239–242.
(23) Towbin, H.; Staehelin, T.; Gordon, J. Electrophoretic Transfer of Proteins from Polyacrylamide Gels to Nitrocellulose Sheets: Procedure and Some Applications. *Proc. Natl. Acad. Sci. U.S.A.* **1979**, *76* (9), 4350–4354.
(24) Brooke, D.; Movahed, N.; Bothner, B. Universal Buffers for Use in Biochemistry and Biophysical Experiments. *AIMS Biophys.* **2015**, *2* (3), 336–342.
(25) Deshpande, M. V.; Eriksson, K.-E.; Göran Pettersson, L. An Assay for Selective Determination of Exo-1,4,-β-Glucanases in a Mixture of Cellulolytic Enzymes. *Anal. Biochem.* **1984**, *138* (2), 481–487.
(26) Zhao, L.; Xie, J.; Zhang, X.; Cao, F.; Pei, J. Overexpression and Characterization of a Glucose-Tolerant β-Glucosidase from *Thermotoga thermarum* DSM 5069T with High Catalytic Efficiency of Ginsenoside Rb1 to Rd. *J. Mol. Catal. B: Enzym.* **2013**, *95*, 62–69.
(27) Bi, Y.; Zhu, C.; Wang, Z.; Luo, H.; Fu, R.; Zhao, X.; Zhao, X.; Jiang, L. Purification and Characterization of a Glucose-Tolerant β-Glucosidase from Black Plum Seed and Its Structural Changes in Ionic Liquids. *Food Chem.* **2019**, *274*, 422–428.
(28) Ariaeenejad, S.; Nooshi-Nedamani, S.; Rahban, M.; Kavousi, K.; Pirbalooti, A. G.; Mirghaderi, S.; Mohammadi, M.; Mirzaei, M.; Salekdeh, G. H. A Novel High Glucose-Tolerant β-Glucosidase: Targeted Computational Approach for Metagenomic Screening. *Front. Bioeng. Biotechnol.* **2020**, *8*, No. 813.
(29) Johnson, K. A.; Goody, R. S. The Original Michaelis Constant: Translation of the 1913 Michaelis–Menten Paper. *Biochemistry* **2011**, *50* (39), 8264–8269.
(30) Natale, P.; Brüser, T.; Driessen, A. J. M. Sec- and Tat-Mediated Protein Secretion across the Bacterial Cytoplasmic Membrane—Distinct Translocases and Mechanisms. *Biochim. Biophys. Acta, Biomembr.* **2008**, *1778* (9), 1735–1756.
(31) Nguyen, K. H. V.; Dao, T. K.; Nguyen, H. D.; Nguyen, K. H.; Nguyen, T. Q.; Nguyen, T. T.; Nguyen, T. M. P.; Truong, N. H.; Do, T. H. Some Characters of Bacterial Cellulases in Goat's Rumen Elucidated by Metagenomic DNA Analysis and the Role of Fibronectin 3 Module for Endoglucanase Function. *Anim. Biosci.* **2021**, *34* (5), 867–879.
(32) Sidar, A.; Voshol, G. P.; Arentshorst, M.; Ram, A. F. J.; Vijgenboom, E.; Punt, P. J. Deciphering Domain Structures of Aspergillus and Streptomyces GH3-β-Glucosidases: A Screening System for Enzyme Engineering and Biotechnological Applications. *BMC Res. Notes* **2024**, *17* (1), No. 257.
(33) Varghese, J. N.; Hrmova, M.; Fincher, G. B. Three-Dimensional Structure of a Barley β-D-Glucan Exohydrolase, a Family 3 Glycosyl Hydrolase. *Structure* **1999**, *7* (2), 179–190.

https://doi.org/10.1021/acsagscitech.5c01090
ACS Agric. Sci. Technol. XXXX, XXX, XXX-XXX

(34) Pyeon, H.-M.; Lee, Y.-S.; Choi, Y.-L. Cloning, Purification, and Characterization of GH3 β-Glucosidase, MtBgl85, from *Microbulbifer thermotolerans* DAU221. *PeerJ* **2019**, *7*, No. e7106.
(35) Serra, G. M.; Siqueira, A. S.; De Molfetta, F. A.; Santos, A. V.; Xavier, L. P. In Silico Analysis of a GH3 β-Glucosidase from Microcystis Aeruginosa CACIAM 03. *Microorganisms* **2023**, *11* (4), No. 998.
(36) Bhatia, Y.; Mishra, S.; Bisaria, V. S. Purification and Characterization of Recombinant *Escherichia coli*-Expressed *Pichia etchellsii* β-Glucosidase II with High Hydrolytic Activity on Sophorose. *Appl. Microbiol. Biotechnol.* **2005**, *66* (5), 527–535.
(37) Turner, P.; Svensson, D.; Adlercreutz, P.; Karlsson, E. A Novel Variant of *Thermotoga neapolitana* β-Glucosidase B Is an Efficient Catalyst for the Synthesis of Alkyl Glucosides by Transglycosylation. *J. Biotechnol.* **2007**, *130* (1), 67–74.
(38) Del Pozo, M. V.; Fernández-Arrojo, L.; Gil-Martínez, J.; Montesinos, A.; Chernikova, T. N.; Nechitaylo, T. Y.; Waliszek, A.; Tortajada, M.; Rojas, A.; Huws, S. A.; Golyshina, O. V.; Newbold, C. J.; Polaina, J.; Ferrer, M.; Golyshin, P. N. Microbial β-Glucosidases from Cow Rumen Metagenome Enhance the Saccharification of Lignocellulose in Combination with Commercial Cellulase Cocktail. *Biotechnol. Biofuels* **2012**, *5* (1), 73.
(39) Bronnenmeier, K.; Staudenbauer, W. L. Purification and Properties of an Extracellular β-Glucosidase from the Cellulolytic Thermophile Clostridium Stercorarium. *Appl. Microbiol. Biotechnol.* **1988**, *28* (4−5), 380–386.
(40) Lee, D.; Kim, T.-J. Characterization of Low-Temperature Enzymatic Reactions through Heterologous Expression and Functional Analysis of Two Beta-Glucosidases from the Termite Symbiotic Bacterium *Elizabethkingia miricola* Strain BM10. *J. Korean Wood Sci. Technol.* **2023**, *51* (4), 270–282.
(41) Alves, L. D. F.; Meleiro, L. P.; Silva, R. N.; Westmann, C. A.; Guazzaroni, M.-E. Novel Ethanol- and 5-Hydroxymethyl Furfural-Stimulated β-Glucosidase Retrieved From a Brazilian Secondary Atlantic Forest Soil Metagenome. *Front. Microbiol.* **2018**, *9*, No. 2556.
(42) O'Sullivan, L. A. Culturable Phylogenetic Diversity of the Phylum "Bacteroidetes" from River Epilithon and Coastal Water and Description of Novel Members of the Family Flavobacteriaceae: *Epilithonimonas tenax* Gen. Nov., Sp. Nov. and *Persicivirga xylanidelens* Gen. Nov., Sp. Nov. *Int. J. Syst. Evol. Microbiol.* **2006**, *56* (1), 169–180.
(43) Ayala, M.; Segovia, C.; Rojas, R.; Miranda, C.; Santander, J. Draft Genome Sequence of *Epilithonimonas* Sp. FP211-J200, Isolated from an Outbreak Episode on a Rainbow Trout (*Oncorhynchus mykiss*) Farm. *Genome Announce.* **2017**, *5* (37), No. e00819-17.
(44) Zhao, X.; Huang, Y.; Ouyang, B.; Wang, G.; Zhang, N.; Zuo, J. Recent Advances in β-Glucosidase Engineering: A Brief Review. *Biol. Life Sci.* June 5, **2023**, DOI: 10.20944/preprints202306.0235.v1.
(45) Erkanli, M. E.; El-Halabi, K.; Kim, J. R. Exploring the Diversity of β-Glucosidase: Classification, Catalytic Mechanism, Molecular Characteristics, Kinetic Models, and Applications. *Enzyme Microb. Technol.* **2024**, *173*, No. 110363.
(46) Ouyang, B.; Wang, G.; Zhang, N.; Zuo, J.; Huang, Y.; Zhao, X. Recent Advances in β-Glucosidase Sequence and Structure Engineering: A Brief Review. *Molecules* **2023**, *28* (13), No. 4990.
(47) Bockwoldt, J. A.; Ehrmann, M. A. Characterisation of Recombinant GH 3 β-Glucosidase from β-Glucan Producing *Levilactobacillus brevis* TMW 12112. *Antonie Van Leeuwenhoek* **2022**, *115* (8), 955–968.
(48) He, Y.; Wang, C.; Jiao, R.; Ni, Q.; Wang, Y.; Gao, Q.; Zhang, Y.; Xu, G. Biochemical Characterization of a Novel Glucose-Tolerant GH3 β-Glucosidase (Bgl1973) from *Leifsonia* Sp ZF2019. *Appl. Microbiol. Biotechnol.* **2022**, *106* (13−16), 5063–5079.
(49) Xie, Y.; Yan, X.; Li, C.; Wang, S.; Jia, L. Characterization and Insight Mechanism of an Acid-Adapted β-Glucosidase from *Lactobacillus paracasei* and Its Application in Bioconversion of Glycosides. *Front. Bioeng. Biotechnol.* **2024**, *12*, No. 1334695.
(50) Zhao, W.; Peng, R.; Xiong, A.; Fu, X.; Tian, Y.; Yao, Q. Expression and Characterization of a Cold-Active and Xylose-Stimulated β-Glucosidase from Marinomonas MWYL1 in *Escherichia coli*. *Mol. Biol. Rep.* **2012**, *39* (3), 2937–2943.
(51) Pengthaisong, S.; Piniello, B.; Davies, G. J.; Rovira, C.; Ketudat Cairns, J. R. Reaction Mechanism of Glycoside Hydrolase Family 116 Utilizes Perpendicular Protonation. *ACS Catal.* **2023**, *13* (9), 5850–5863.
(52) Wang, C.; Yang, Y.; Ma, C.; Sunkang, Y.; Tang, S.; Zhang, Z.; Wan, X.; Wei, Y. Expression of β-Glucosidases from the Yak Rumen in Lactic Acid Bacteria: A Genetic Engineering Approach. *Microorganisms* **2023**, *11* (6), No. 1387.
(53) Salgado, J. C. S.; Meleiro, L. P.; Carli, S.; Ward, R. J. Glucose Tolerant and Glucose Stimulated β-Glucosidases – A Review. *Bioresour. Technol.* **2018**, *267*, 704–713.
(54) Srivastava, N.; Rathour, R.; Jha, S.; Pandey, K.; Srivastava, M.; Thakur, V. K.; Sengar, R. S.; Gupta, V. K.; Mazumder, P. B.; Khan, A. F.; Mishra, P. K. Microbial Beta Glucosidase Enzymes: Recent Advances in Biomass Conversation for Biofuels Application. *Biomolecules* **2019**, *9* (6), No. 220.
(55) Yang, X.; Ma, R.; Shi, P.; Huang, H.; Bai, Y.; Wang, Y.; Yang, P.; Fan, Y.; Yao, B. Molecular Characterization of a Highly-Active Thermophilic β-Glucosidase from *Neosartorya f.ischeri* P1 and Its Application in the Hydrolysis of Soybean Isoflavone Glycosides. *PLoS One* **2014**, *9* (9), No. e106785.
(56) Na Takuathung, M.; Teekachunhatean, S.; Chansakaow, S.; Klinjan, P.; Inpan, R.; Kongta, N.; Tipduangta, P.; Tipduangta, P.; Dukaew, N.; Sakuludomkan, C.; Koonrungsesomboon, N. The Effects of SOY Extract Nutraceuticals on Postmenopausal Women's Health: A Randomized, Double-Blind, Placebo-Controlled Trial. *J. Funct. Foods* **2024**, *113*, No. 106055.
(57) Hassan, F.; Arshad, M. A.; Li, M.; Rehman, M. S.; Loor, J. J.; Huang, J. Potential of Mulberry Leaf Biomass and Its Flavonoids to Improve Production and Health in Ruminants: Mechanistic Insights and Prospects. *Animals* **2020**, *10* (11), No. 2076.
(58) Kim, D.; Kuppusamy, P.; Jung, J. S.; Kim, K. H.; Choi, K. C. Microbial Dynamics and *In Vitro* Degradation of Plant Secondary Metabolites in Hanwoo Steer Rumen Fluids. *Animals* **2021**, *11* (8), No. 2350.
(59) Maffucci, I.; Laage, D.; Sterpone, F.; Stirnemann, G. Thermal Adaptation of Enzymes: Impacts of Conformational Shifts on Catalytic Activation Energy and Optimum Temperature. *Chem. Eur. J.* **2020**, *26* (44), 10045–10056.
(60) Sestelo, A. B. F.; Poza, M.; Villa, T. G. β-Glucosidase Activity in a *Lactobacillus plantarum* Wine Strain. *World J. Microbiol. Biotechnol.* **2004**, *20* (6), 633–637.
(61) Mesas, J. M.; Rodríguez, M. C.; Alegre, M. T. Basic Characterization and Partial Purification of β-Glucosidase from Cell-Free Extracts of *Oenococcus oeni* ST81: β-Glucosidase from *Oenococcus oeni* ST81. *Lett. Appl. Microbiol.* **2012**, *55* (3), 247–255.
(62) Florindo, R. N.; Souza, V. P.; Manzine, L. R.; Camilo, C. M.; Marana, S R; Polikarpov, I.; Nascimento, A. S. Structural and Biochemical Characterization of a GH3 β-Glucosidase from the Probiotic Bacteria *Bifidobacterium adolescentis*. *Biochimie* **2018**, *148*, 107–115.
(63) Teugjas, H.; Väljamäe, P. Selecting β-Glucosidases to Support Cellulases in Cellulose Saccharification. *Biotechnol. Biofuels* **2013**, *6* (1), No. 105.
(64) De Giuseppe, P. O.; Souza, T. D. A. C. B.; Souza, F. H. M.; Zanphorlin, L. M.; Machado, C. B.; Ward, R. J.; Jorge, J. A.; Furriel, R. D. P. M.; Murakami, M. T. Structural Basis for Glucose Tolerance in GH1 β-Glucosidases. *Acta Crystallogr. D: Biol. Crystallogr.* **2014**, *70* (6), 1631–1639.
(65) Monteiro, L. M. O.; Vici, A. C.; Pinheiro, M. P.; Heinen, P. R.; De Oliveira, A. H. C.; Ward, R. J.; Prade, R. A.; Buckeridge, M. S.; Polizeli, M. D. L. T. D. M. A Highly Glucose Tolerant ß-Glucosidase from Malbranchea pulchella (MpBg3) Enables Cellulose Saccharification. *Sci. Rep.* **2020**, *10* (1), No. 6998.

https://doi.org/10.1021/acsagscitech.5c01090
ACS Agric. Sci. Technol. XXXX, XXX, XXX-XXX